# Optimization of inter-subband absorption of InGaAsSb/GaAs quantum wells structure

Lynda Chenini, Abdelkader Aissat, Jean-Pierre Vilcot

Version of Record: https://www.sciencedirect.com/science/article/pii/S0749603619300618
Manuscript_ebf5b4ecf801cf079ed3fcaf9368c4c7

# Optimization of Inter-subband Absorption of InGaAsSb/GaAs Quantum Wells Structure

L. Chenini[a], A. Aissat[a, b] and J.P.Vilcot[b]

[a] Faculty of Technology, University of Blida 1, ALGERIA
[b] Institut d'Electronique, de Microélectronique et de Nanotechnologie (IEMN), UMR 8520, Université des Sciences et Technologies de Lille 1, Avenue Poincaré, CS60069,
59652 Villeneuve d'Ascq, France

## Abstract

In this work, we theoretically investigate the structural dependence of intersubband absorption of InGaAsSb/GaAs single quantum well structures. We begin by analyzing the impact of In and Sb incorporation on the critical thickness, conduction band offset and band gap energy. The first two electron energy levels $E_{12}$ and the corresponding wavelength were made for the $In_xGa_{1-x}As_{1-y}Sb_y$/GaAs system and are analyzed in detail by solving the Schrödinger equation. Also, we have investigated effects of composition and well width on the intersubband absorption. In addition, the wavelength and absorption coefficient of the ISBT can be adjusted and optimized by changing the composition and the width of the SQW. Finally, strain effects on intersubband absorption and on the peak response wavelength have also been systematically studied. Our study shows that InGaAsSb/GaAs SQW will play a key role in research of electronics and photonic devices in the future.

***Keywords*:** InGaAsSb/GaAs SQW, intersubband transition, conduction band, absorption, cascade laser

## 1. Introduction

During the last decade, the study of intersubbands transitions in quantum wells has been an interesting subject of investigation. It consists of only one type of carrier (unipolar semiconductor laser) and on electronic transitions between conduction band states (or valence band states) occurring by the size quantization in semiconductor heterostructures as we can see in figure 1.This great interest is due to their important and fundamental characteristics as: a large dipole moment, an ultra-fast relaxation time, and an outstanding tunability of the transition wavelengths [1].These phenomena have shown advanced applications in optoelectronic and microelectronic devices and allowed appearance of many important devices such as: far- and near-infrared photodetectors [2, 3], ultrafast all-optical modulators [4], all optical switches [5],quantum cascade lasers [6,7] and quantum well infrared detectors [8, 9].One had to wait for the many improvements in growth techniques to observe intersubband emissions in III-V materials [10,11].Among them, the Sb based heterostructures which have a great interest in many applications such as environmental protection, remote sensing of atmospheric and optical communication, more other applications are cited in the references[12-16]. Several theoretical studies on

the absorption coefficient associated with intersubband optical transitions in single-QWs and multiple-QW structures are presented in the literature [17-20]. However, very limited investigations have been carried out on intersubband transition in lattice matched InGaAsSb/GaAs quantum well [21-23].

In this work, we investigate the absorption coefficients and wavelength of the ISBT of the $In_xGa_{1-x}As_{1-y}Sb_y$/GaAs single quantum well. The absorption coefficient of the ISBT can be determined by three factors which are: the modulus square of dipole matrix, the total electrons residing in the initial and final subbandand the energy distance between these two subbands. In this study, the influence of quantum well thickness, composition ($x$, $y$) and strain on the absorption coefficients and the wavelength of the ISBT in a single $In_xGa_{1-x}As_{1-y}Sb_y$/GaAs well have been studied by solving the Schrödinger equation. With this aim, it is very important to determine in a first step the electronic properties of strained $In_xGa_{1-x}As_{1-y}Sb_y$/GaAs SQW, such as critical thickness, band gap, and band discontinuities as a function of the structural parameters. It is worth citing that this study is an approximation since complexity is not included. In the present simple approach, the ISBTs are related to subbands only. The analysis is restricted here to the case of absorption from the fundamental level to the excited one. So, only photons with some vertical component along the growth axis of the electric field can induce ISBTs.

The paper is organized as follows, after a brief introduction; we describe in section 2 the theoretical calculations. The obtained results on the electronic properties for $In_xGa_{1-x}As_{1-y}Sb_y$/GaAs and absorption coefficient as a function of structural parameters are reported in section 3. Conclusions are summarized in section 4.

An example of $In_{0.35}Ga_{0.65}As_{0.97}Sb_{0.03}$/GaAs single quantum well structure is given in figure 2. The figure indicates the values of band gap energy, band alignment, resulting energy levels for electrons and holes and the thickness of each layer of the QW. The compressive strain is $\varepsilon_{xx}$=2.67%. $E_{12}$ is the transition energy between the two first electron subband energies ($E_1$ and $E_2$).

## 2. Theoretical model

The absorption coefficient peak position depends on the subband energy position and intersubband energy difference in the wells. To study the energy levels of lattice matched InGaAsSb/GaAs quantum well, we must solve analytically the Schrodinger equation [24]:

$$\left(-\frac{\hbar^2}{2m^*}\frac{\partial^2}{\partial z^2}+V(z)\right)\psi_i(z)=\mathrm{E}_i\psi_i(z) \quad (1)$$

where

$\psi$: the envelope function,

$\hbar$: reduced Planck constant,

$m^*$: electron effective mass in the conduction band,

$V(z)$: conduction band potential,

$i$ the subband index and $E_i$ subband energies in the conduction band.

The solution of Schrödinger equation gives us the following expression:

$$\frac{\sqrt{2m^*_{InGaAsSb}E_i}}{\hbar}L_w = n\pi - 2arctg\left(\sqrt{\frac{m^*_{GaAs}E_i}{m^*_{InGaAsSb}(V-E_i)}}\right) \quad (2)$$

where $m^*_{InGaAsSb}$ and $m^*_{GaAs}$are the electron effective mass in quantum well and barrier, respectively.

Knowing the transition rate between two subbands $n$ and $m$, given as $E_{nm} = E_n - E_m$, gives us the possibility to calculate corresponding wavelength which can be expressed as:

$$\lambda = \frac{1.24}{E_{nm}(eV)} \quad (3)$$

Where: $E_n$ and $E_m$ are the quantized energies of subbands $n$ and $m$, respectively. After solving the Schrodinger equation, we calculate the Fermi energy and electron population of each energy state in order to be able to calculate the ISBT coefficient.

The intersubband absorption coefficient depends on the momentum matrix element, the incident photon wavelength and the difference in the subband density of electrons in the ground state ($E_n$) and the first excited state ($E_m$) as mentioned in the following equation [25, 26]:

$$\alpha_{nm}(h\nu) = \frac{\pi e^2}{nc\varepsilon_0 m_0^2 \omega}\frac{2}{V}\sum|M_{nm}|^2(f_n - f_m) \times \Gamma/\left[(E_n - E_m - h\nu)^2 + (\pi\Gamma)^2\right] \quad (4)$$

where

$e$: the electron charge,

$n$: the refractive index,

$c$: the speed of light,

$\varepsilon_0$: the free-space dielectric constant,

$\nu$: the photon frequency,

$V$ is the space volume,

$M_{nm}$ is the momentum matrix element between subbands $n$ and $m$, $f_n$ and $f_m$ are the Fermi-Dirac distributions of electrons in respective subbands, $\Gamma = \frac{\hbar}{\tau\pi}$ and $\tau$ is the relaxation time, we assume that the relaxation time is constant and is taken as $\tau$= 0.1 ps.

Along the z direction, the momentum matrix is given by:

$$M_{nm} = \int_{-L_W/2}^{L_W/2} \psi_n^*(z) z \psi_m(z) dz \quad (5)$$

Where $\psi_j(z)$ is the wave function of the $j^{th}$ subband with $j$=($n$,$m$), obtained by solving the Schrödinger equation. The total amount of electrons residing in the $j^{th}$ subband level can be obtained by:

$$n(z) = \sum_j \left|\psi_j(z)\right|^2 n_j \quad (6)$$

Where $n_j$, the sheet density of electrons of $j^{th}$ subband, given by:

$$n_j = \frac{m^* k_B T}{\pi\hbar^2} ln\left[1 + exp\left(\frac{E_F - E_j}{k_B T}\right)\right] \quad (7)$$

Where $k_B$ is the Boltzmann's constant, $T$ is the temperature, $E_j$ are energy at $j^{th}$ eigenstates and $E_F$ is the Fermi level in the conduction band.

The oscillator strength $f_{nm}$ of intersubband absorption in the InGaAsSb/GaAs quantum well for the incident photon energy depends on the momentum matrix element and transition energy $E_{nm}$ as mentioned in equation (8).

$$f_{nm} = \frac{2m_0}{\hbar^2} |M_{nm}|^2 (E_n - E_m) \quad (8)$$

The band parameters of the parental binary compounds used in our study are taken from Ref [27] and are interpolated according to the Vegard's law except the band gap energy. An equation similar to that taken from reference [28] is used.

$$E_g(x,y) = xE_{GaAsSb}(y) + (1-x)E_{InAsSb}(y) - \Delta E \quad (9)$$

where

$$\Delta E = x(1-x)[yC_{InGaSb} + (1-y)C_{InGaAs}] + y(1-y)[xC_{GaAsSb} + (1-x)C_{InAsSb}] \quad (10)$$

$E_{GaAsSb}, E_{InAsSb}, C_{InGaSb}, E_{InGaAs}, E_{GaAsSb}, E_{InAsSb}$, are band gap and bowing parameters of the corresponding ternaries constituent, respectively.

The effect of strain is taken into account. For a strained-layer quantum well grown along the [100] axis (growth direction is taken to be the z axis), the strain tensor is diagonal, with the following non-zero components $\varepsilon_{xx} = \varepsilon_{yy} = \varepsilon_{//}$ and $\varepsilon_{zz} = \varepsilon_{\perp}$. Both parallel $\varepsilon_{//}$and perpendicular strain $\varepsilon_{\perp}$ can be defined as follows:

$$\varepsilon_{//} = \frac{a_{GaAs} - a_{InGaAsSb}}{a_{InGaAsSb}} \tag{11}$$

$$\varepsilon_{\perp} = -2\frac{C_{12}^{InGaAsSb}}{C_{11}^{InGaAsSb}}\varepsilon_{//} \tag{12}$$

Where: $a_{GaAs}$ and $a_{InGaAsSb}$ are the lattice constants of the substrate which is assumed to be GaAs and the layer quantum well, respectively, $C_{11}^{InGaAsSb}$and $C_{12}^{InGaAsSb}$are the stiffness constantsof quaternary alloy, they depend on the concentration ($x$, $y$) and are obtained by interpolation as mentioned before. The knowledge of the discontinuities for conduction bands at the strained and lattice-matched interfaces is essential to control the carrier transport and analysis of electronic properties. The model-solid approach of Van de Walle and Martin is widely used for determining the extrema of energy bands [29].

The conduction band offset is expressed as the difference:

$$\Delta E_c = E_c^b - E_c^w \tag{13}$$

Where $E_c^b$ and $E_c^w$ are the conduction bands of barrier and well, respectively.

The estimates of the critical thicknesses may serve as guideline for the choice of the well width $L_w$ and composition ($x$, $y$) of strained InGaAsSb/GaAs QWs suitable for light emission in important spectral ranges and free from stress relaxation. So, critical thickness knowledge is important key in growth processing of high quality semiconductor heterostructures and to achieve high performance of the optoelectronic devices.

The theoretical expression, proposed by Matthews and Blakeslee [30] to account for the critical layer thickness is used in this work and is defined as:

$$h_c = \frac{a(1-0.25.\nu)}{2\sqrt{2}\pi(1+\nu)\varepsilon_{xx}}\left[ln\left(\frac{\sqrt{2}h_c}{a}\right)+1\right] \tag{14}$$

$\nu$is the Poisson's ratio:

$$\nu = \frac{C_{12}}{C_{11}+C_{12}} \tag{15}$$

## 3. Results and discussion

Figure 3 presents the results of a critical thickness calculation of an $In_xGa_{1-x}As_{1-y}Sb_y$epilayer grown on GaAs substrate. The critical thickness strongly depends on the indium and antimony composition. It decreases as indium and antimony contents increase. Figure 4 describes the CB offset variation as a function of indium ($x$) and antimony ($y$) fractions in minimum Γ according to the model solid theory.We note that the CBO are positive over the whole range of the composition. It should be noted also from this figure that larger $\Delta E_c$ values can be obtained by increasing In and Sb contents. Next, we have calculated the band gap energy of $In_xGa_{1-x}As_{1-y}Sb_y$/GaAs as mentioned in section 2. The results are plotted in figure 5 in the form of contour plots versus In and Sb. Addition of a small quantity of both Sb and In leads to a decrease of band gap energy. Figure 6 shows the transition energy evolution $E_{12}$as a function of thickness well for several Sb concentrations of $In_{0.15}Ga_{0.85}As_{1-y}Sb_y$/GaAs SQW. At first, the transition energy $E_{12}$ increases with $L_w$ and reaches the climax when $L_w$ is equal to a value that will be named $L_{wm}$. However, when $L_w$ is larger than $L_{wm}$, the ISBT energy decreases. This can be explained as follows: When $L_w$ is smaller than $L_{wm}$, the energy distance between the two first subbands 1 and 2 decreases with $L_w$, and the total electrons located in first subband decrease with $L_w$, where, the electron density in second subband is negligible. Therefore, the difference between electron densities in subbands 1 and 2 is mainly determined by those of first subband. The decrease of the energy distance exceeds the decrease of total electrons locating in subband 1 when $L_w$ is smaller than $L_{wm}$, which leads to increasing the ISBT with $L_w$. However, with increasing $L_w$, the total electrons locating in the first subband decrease so quickly, that it becomes the prevailing factor, which leads to decrease the ISBT with increasing $L_w$. It is also seen from figure 6 that with increasing antimony concentration intersubband energy $E_{12}$ blueshift. The inset shows calculated intersubband energy $E_{12}$ of $In_xGa_{1-x}As_{0.98}Sb_{0.02}$/GaAs as a function of well width for different indium values. Indium has a strong effect on transition energy. Transition energy blueshift when indium content increases. Figure 7 shows the wavelength of the $E_{12}$ ISBT as a function of well width for different Sb fractions. The inset shows the wavelength of the $E_{12}$ ISBT as a function of well width for different percentages of Indium. Moreover, the intersubbands operating wavelength is much more sensitive to both, contents and well width. Figure 8 presents the absorption coefficients of 1–2 ISBT as a function of the wavelength for different indium concentrations of the 70 Å $In_xGa_{1-x}As_{0.075}Sb_{0.025}$/GaAs quantum well at room temperature. As indium content

increases, the absorption coefficient gradually increases too. Figure 8 clearly shows that the range wavelength of emission shifts to shorter wavelengths and the spectral linewidth became narrower. Figures 9 and 10 show the absorption spectra versus wavelength for the InGaAsSb/GaAs structure with $L_w$=60 Å at room temperature. The calculations are down for different values of Antimony varying from 0.5 to 4% and $x$=25%. It is found that the absorption coefficients of 1–2 ISBT decrease with Sb content. The wavelength of 1–2 ISBT decreases with Sb at first, reaches its minimum value equal to 10.2 µm (121.6 meV) when Sb=1.9-2% and then increases with Sb. The absorption coefficient is plotted as a function of wavelength in figure 11 for different well widths ranged from 40 to 90Åfor the $In_{0.20}Ga_{0.80}As_{0.98}Sb_{0.02}$/GaAs quantum well structure at T=300K.It is seen from the plot that the absorption coefficient of 1-2 ISBT decreases with $L_w$. Increasing well width modifies the geometric confinement of the electrons which varies the subband dispersion relations and leads to an alteration in the overlap function between the first and second subband. The energy levels of both subband 1 and subband 2 decreases with increasing $L_w$. But, the energy level of subband 2 decreases more slowly than that of subband 1 before $L_w$ exceeds 60Å. Therefore, the energy distance between subbands 1 and 2 will increase with $L_w$, which means that the wavelength of ISBT between subbands 1 and 2 decreases with increasing $L_w$. when $L_w$ is larger than 60 Å, the energy level of subband 2 decreases more quickly than that of subband 1, thus the energy distance between subbands 1 and 2 decreases with $L_w$, and the wavelength of ISBT between subbands 1 and 2 increases with increasing $L_w$. However, the absorption coefficient of ISBT $E_2$–$E_1$ is blue shifted for well widths less than 60Å but above this value it redshifts. The spectral linewidth became narrower for well widths less than 60 Å while it becomes wider above this value. Figure 12 shows the variation of peak response wavelength (left) and absorption peak positions(right)as a function of compressive strain. It can be found that the peak value of absorption coefficient is directly related to strain, and, simultaneously, the absorption maximum shifts to shorter wavelengths. The peak response wavelength decreases from 28.55 to 8.98 µm as the compressive strain increases from 0.69 to 2.97%. Similarly, the maximum absorption increases from 748.8 to 3990 $cm^{-1}$.

## 4. Conclusion

In conclusion, intersubband absorption coefficient characteristics and its dependence on the structural parameters are theoretically investigated for strained $In_xGa_{1-x}As_{1-y}Sb_y$/GaAs quantum well structure. Both, In and Sb have significant impact on electronic properties. We have analytically solved the Schrodinger equation as well as the intersubband absorption coefficient. According to the results of this study, we have deduced that: i) The variation

in the structural parameters can tune the energy subband positions and consequently the intersubband in the well to guarantee maximum absorption; ii) The intersubbands optical absorption increases when indium concentration increases. The range wavelength of emission shifts to shorter wavelengths and the spectral linewidth became narrower; iii) The absorption peaks decreases when antimony increases and they shift to short wavelength for a value less than 1.9-2%, but above these values they shift to longer wavelengths; iv) The absorption peaks decrease when well width increases and they shift to short wavelength for a well width less than 60 Å, but above this value they shift to longer wavelengths. So, changing the structural parameters values vary both the position and peak values of absorption coefficient. v) In this study, we have also examined the effects of compressive strain on the peak response wavelength and absorption peak positions of InGaAsSb/GaAs ISQW. We conclude that compressive strain has a significant influence on both. We see that the peak wavelength decreases when strain increases and its shift to shorter wavelengths while absorption peak positions increases. The results indicate that long wavelength infrared (LWIR) detectors or quantum cascade lasers can be realized by InGaAsSb/GaAs SQW. We expect that our theoretical results will serve as a guideline for future experimental results.

## References


[1] N. Eseanu, Simultaneous effects of laser field and hydrostatic pressure on the intersubband transitions in square and parabolic quantum wells, Phys. Lett. A. 374 (2010) 1278–1285.

[2] F.D.P. Alves, G. Karunasiri, N. Hanson, M. Byloos, H.C. Liu, A. Bezinger, M. Buchanan, NIR, MWIR and LWIR quantum well infrared photodetector using interband and intersubband transitions, Infrared Phys. Technol.50 (2007) 182-186.

[3] S.S. Li, Multi-color, broadband quantum well infrared photodetectors for mid-, long-, and very long wavelength infrared applications, IJHSES. 12 (2002) 761-801.

[4] Y. Li, A. Bhattacharya, C. Thomidis, T.D. Moustakas, R. Paiella, Ultrafast all optical switching with low saturation energy via intersubband transitions in GaN/AlN quantum-well waveguides, Optics Express.15 (2007) 17922- 17927.

[5] N. Iizuka, K. Kaneko, N. Suzuki, All-optical switch utilizing intersubband transition in GaN quantum wells, IEEE I. Quantum Electron.42 (2006) 765-771.

[6] M. A. Belkin, F. Capasso, F. Xie, A. Balyanin, M. Fischer, A. Whitmann, J. Faist, Room temperature terahertz quantum cascade laser source based on intracavity difference-frequency generation, Appl. Phys. Lett. 92 (2008) 201101.1-201101.3

[7] T. Chakraborty, V. M. Apalkov, Quantum cascade transitions in nanostructures, Adv. phys.52 (2003) 455-521.

[8] S.D. Gunapala, S.V. Bandara, J.K. Liu, J.M. Mumolo, S.B. Rafol, D. Z. Ting, A. Soibel, C. Hill, Quantum well infrared photodetector technology and applications, IEEE J. Sel. Top. Quantum. Electron.20 (2014) 3802312.1-3802312.12.

[9] A. Aissat, R. Bestam, B. Alshehri, J. P. Vilcot, Modeling of the absorption properties of $Ga_{1-x}In_xAs_{1-y}N_y$/GaAs quantum well structures for photodetection applications, Superlattices and Microstructures, Volume 82, (2015), 623-629

[10] L. C. West and S. J. Eglash,First observation of an extremely large dipole infrared transition within the conduction band of a GaAs quantum well, J. Appl. Phys. Lett. 46 (1985) 1156–1158.

[11]M. Helm, P. England, E. Colas, F. DeRosa, and S.J. Allen, Intersubband Emission from Semiconductor Superlattices Excited by Sequential Resonant Tunneling, Phys. Rev. Lett. 63 (1989) 74–77.

[12] N.T. Yeh, P.C. Chiu, J.I. Chyi, F. Ren, S.J. Pearton, Sb-based semiconductors for low power electronics,J.Mater. Chem. C.1 (2013) 4616- 4627.

[13] M. W. Dashiell et al, Quaternary InGaAsSb Thermophotovoltaic Diodes, IEEE Trans. Electron. devices. 53 (2006) 2879-2891.

[14]R. A. Arif and N.Tansu, Interdiffused SbN-Based Quantum Well on GaAs for 1300-1550 nm Diode Lasers, Mater.Res. Soc. Symp. Proc.891 (2006) 1-6.

[15] K. H. Su, W. C. Hsu, C. S. Lee, T. Y. Wu, Y. H. Wu, L. Chang, R. S. Hsiao, J. F. Chen, and T. W. Chi, A Novel Dilute Antimony Channel $In_{0.2}Ga_{0.8}$AsSb/GaAs HEMT, IEEE Electr.Device.Lett.28 (2007) 96-99

[16] C. A. Wang and H. K. Choi, GaInAsSb/AlGaAsSb multiple-quantum-well diode lasers grown by organometallic vapor phase epitaxy, Appl. Phys. Lett.70 (1997) 802-804.

[17] Y. Z. Wang, D. Li, L. Li, N. Y. Liu, L. Liu, W. Y. Cao, W. H. Chen, X. D. Hu, Intersubband transitions in $Al_{0.82}In_{0.18}$N/GaN single quantum well, Chin. Phys. B. 20 (2011) 094207.1-094207.6

[18] N. Suzuki, N. Iizuka, K. Kaneko, Calculation of near-infrared intersubband absorption spectra in GaN/AlN quantum wells. Jpn. J. Appl. Phys. 42 (2003) 132–139

[19] A. Rostami, H. RasooliSaghai, H. Baghban AsghariNejad, Defect-induced enhancement of absorption coefficient and electro absorption properties in GaN/AlGaN centered defect quantum box (CDQB) nanocrystal, Physica B: Condensed Matter. 403 (2008) 2789-2769.

[20] S. H. Park, D. Ahn, C. Y. Park, Intersubband transition in lattice-matched BGaN/AlN quantum well structures with high absorption coefficients, Optics Express. 25 (2017) 3143-3152.

[21] M. Motyka, G. Sęk, K. Ryczko, M. Dyksik, R. Weih, G. Patriarche, J. Misiewicz, M. Kamp, S. Höfling, Interface Intermixing in Type II InAs/GaInAsSb Quantum Wells Designed for Active Regions of Mid-Infrared-Emitting Interband Cascade Lasers, Nanoscale Res. Lett. 10 (2015) 1-7.

[22] T. Inoue, M.D. Zoysa, T. Asano, S. Noda, Realization of narrowband thermal emission with optical nanostructures, Optica. 2 (2015) 27-35.

[23] W. Lei, C. Jagadish, Lasers and photodetectors for mid-infrared 2-3 µm applications, J. Appl. Phys.104 (2008) 091101.1-091101.11.

[24] A. Laakso, M. Dumitrescu, L. Toikkanen, A. Tukiainen, V. Rimpiläinen and M. Pessa, Simulation of quantum wells with 'spikes' and 'dips', Opt. Quant. Electro. 40 (2008) 319–324

[25] W. Liu, D. H. Zhang, W. J. Fan, X. Y. Hou, and Z. M. Jiang, Intersubband transitions in InGaAsN/GaAs quantum wells, J. Appl. Phys.104 (2008) 053119.1-053119.8

[26] M. Courel, J. C. Rimada and L. Hernández, "AlGaAs/ GaAs Superlattice Solar Cells," *Progress in Photovoltaics*: *Research and Applications*, Vol. 21, No. 3, (2012) 276-282.

[27] I. Vurgaftman, J.R. Meyer and L.R. Ram-Mohan, Band parameters for III–V compound semiconductors and their alloys,J. Appl. Phys.89 (2001) 5815-5875.

[28] B. W. Gang and L. Aizhen, Band gap energy and its temperature dependence of GaInAsSb quaternary alloy grown by molecular beam epitaxy, Chinese Phys. Lett. 9 (1992) 53-56.

[29] A.Jdidi, N.Sfina, S. Abdi-Ben Nassrallah, M. Saïd and J. L. Lazzari, A multi-color quantum well photodetector for mid- and long-wavelength infrared detection, Semicond. Sci. Technol. 26 (2011) 125019.1-125029

[30] J.W. Matthews, A.E. Blakeslee, Defects in epitaxial multilayers: I. Misfit dislocations, J. Cryst. Growth. 27 (1974) 118-125.

## Figures caption

Figure 1. Conduction Band of the quantum well structure InGaAsSb/GaAs

Figure 2. Quantum confinement potential and energy levels for electrons and holes for a set of 7 nm wide $In_{0.35}Ga_{0.65}As_{0.97}Sb_{0.03}$/GaAsQWs.

Figure 3. Calculated critical thickness ($h_c$) of lnGaAsSb on a GaAs substrate.

Figure 4. Conduction band offset $\Delta E_c$ in minimum Γ of InGaAsSb/GaAs.

Figure 5. Evolution of band gap energy of InGaAsSb/GaAs at room temperature.

Figure 6. The transition energy $E_{12}$ as a function of well width for different values of Sb. The inset shows the transition energy $E_{12}$ as a function of well width for different values of In.

Figure 7.The wavelength of the ISBT between subbands1 and 2as a function of well width for different Sb values. The inset shows the wavelength of the ISBT between subbands1 and 2 as a function of well width for different Invalues.

Figure 8.Variation of the absorption coefficient of 1–2 ISBT with the wavelength for different values of indium.

Figure 9.Variation of the absorption coefficient of 1–2 ISBT with the wavelength for different values of antimony.

Figure 10.Variation of peak response wavelength (blue)and absorption peak positions (red)of InGaAsSb/GaAs QW structure as a function of Sb contents.

Figure 11.Absorption spectra of $In_{0.20}Ga_{0.80}As_{0.98}Sb_{0.02}$ /GaAs structure as a function of wavelength for different well widths.

Figure 12. Effect of compressive strain on the peak response wavelength (left) of InGaAsSb/GaAs QW and the maximum absorption (right).

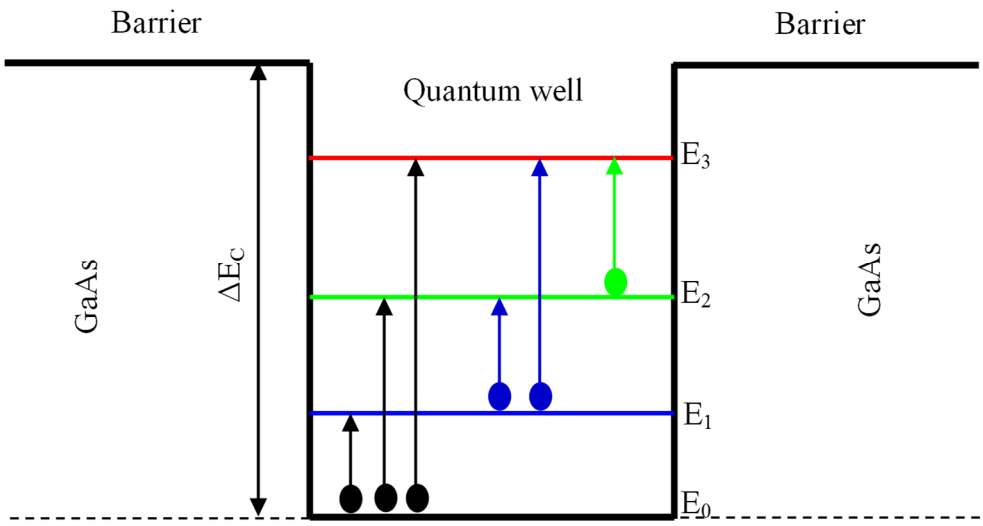


Figure 1

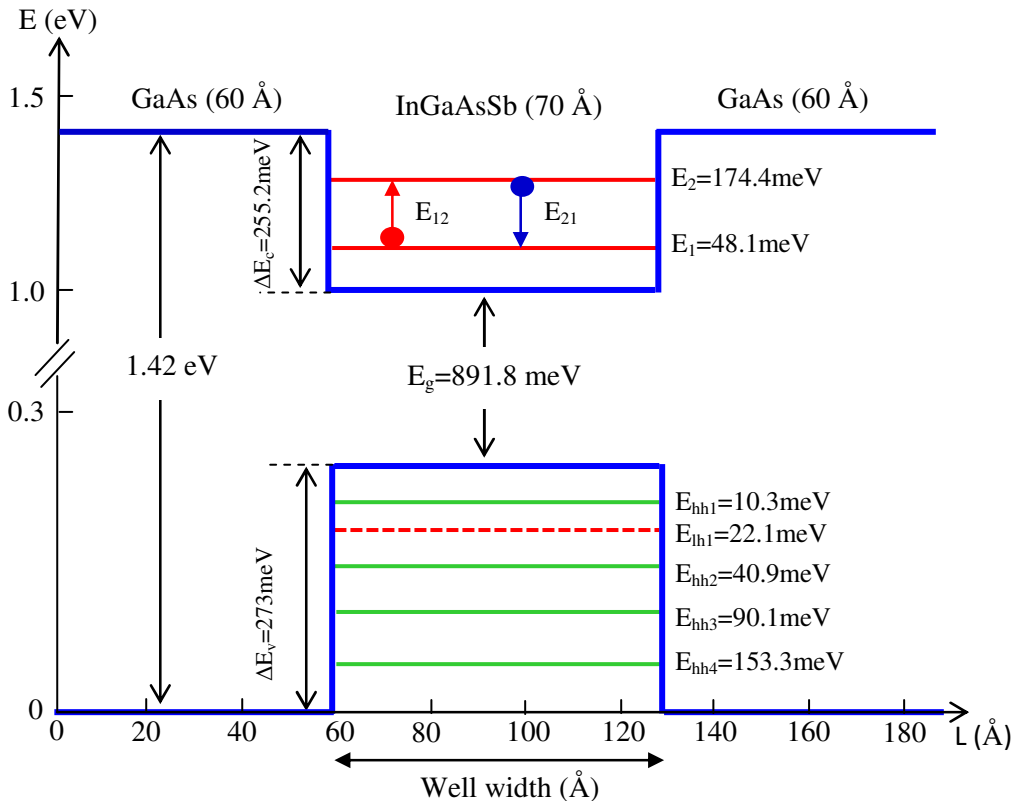


Figure 2

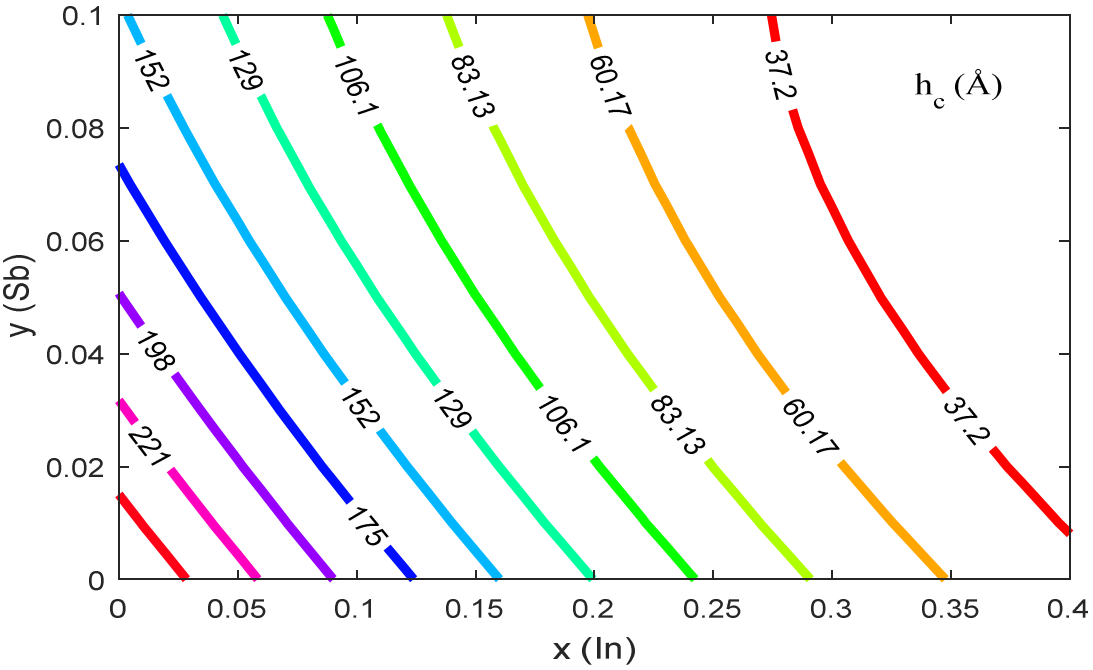


Figure 3

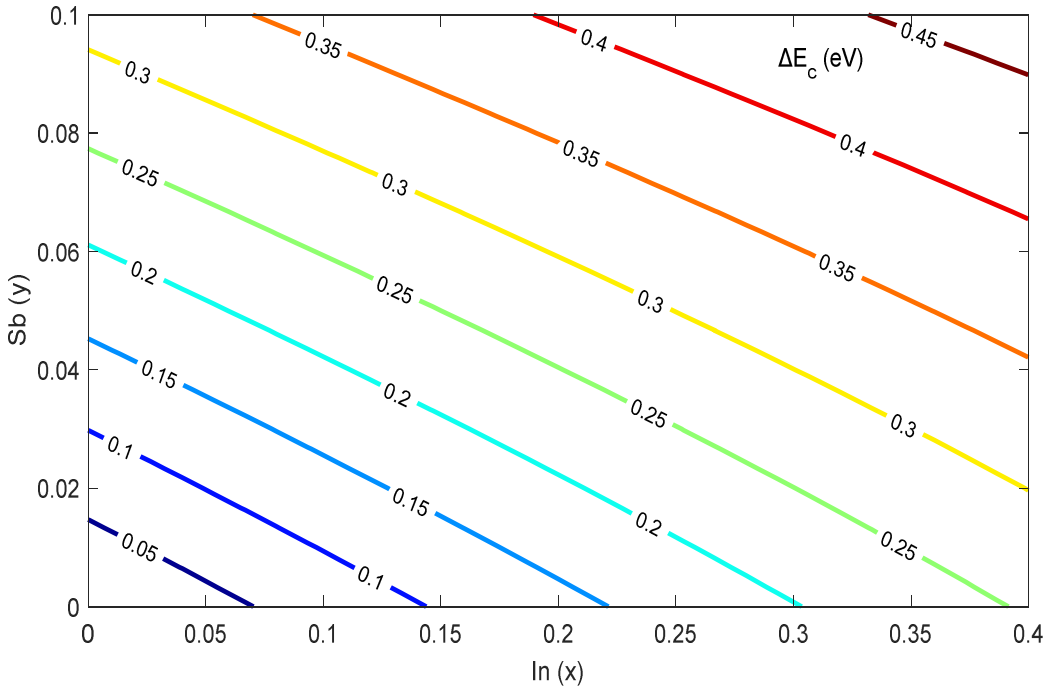


Figure 4

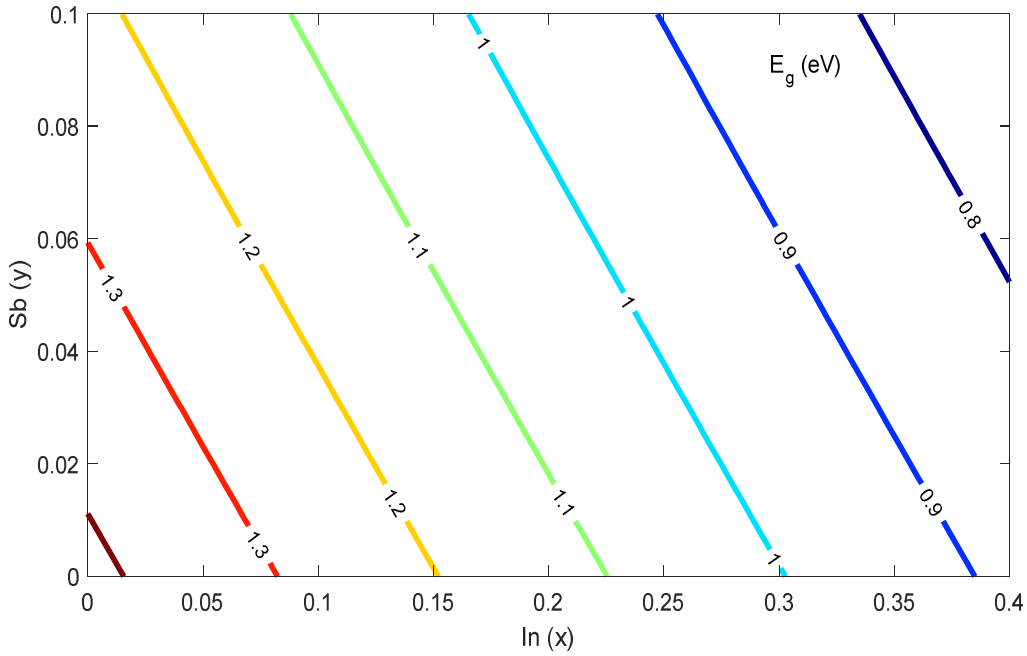


Figure 5

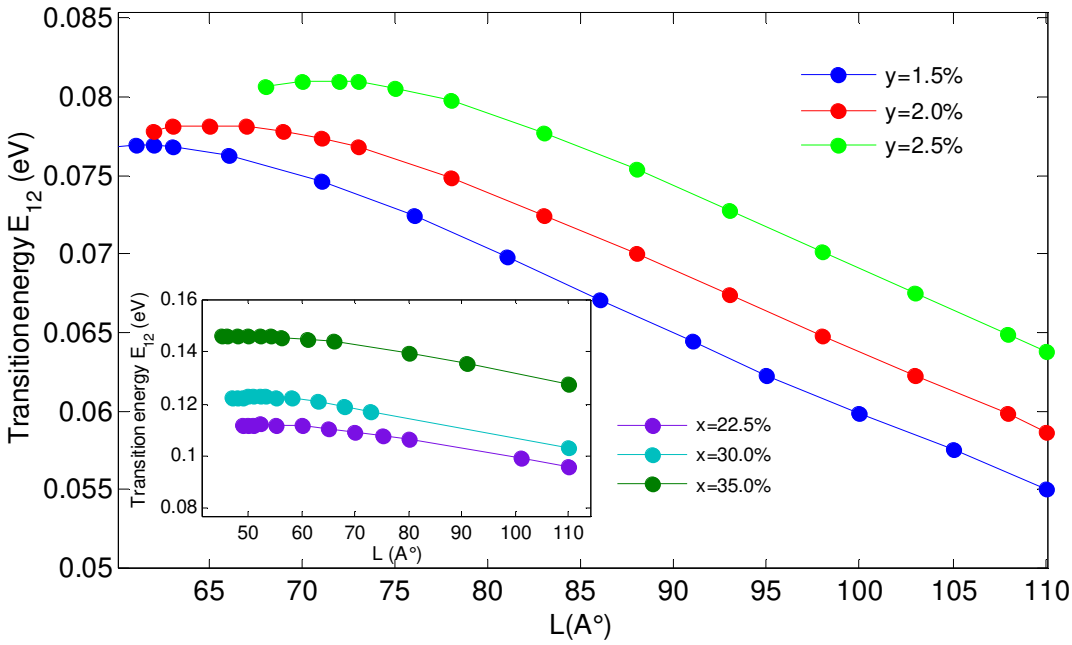


Figure 6

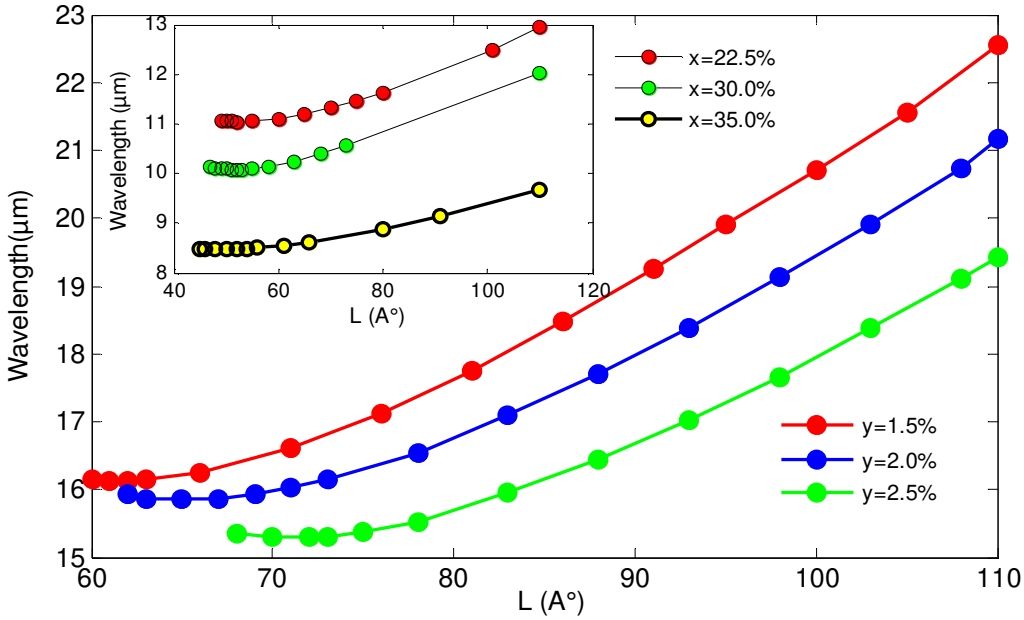


Figure 7

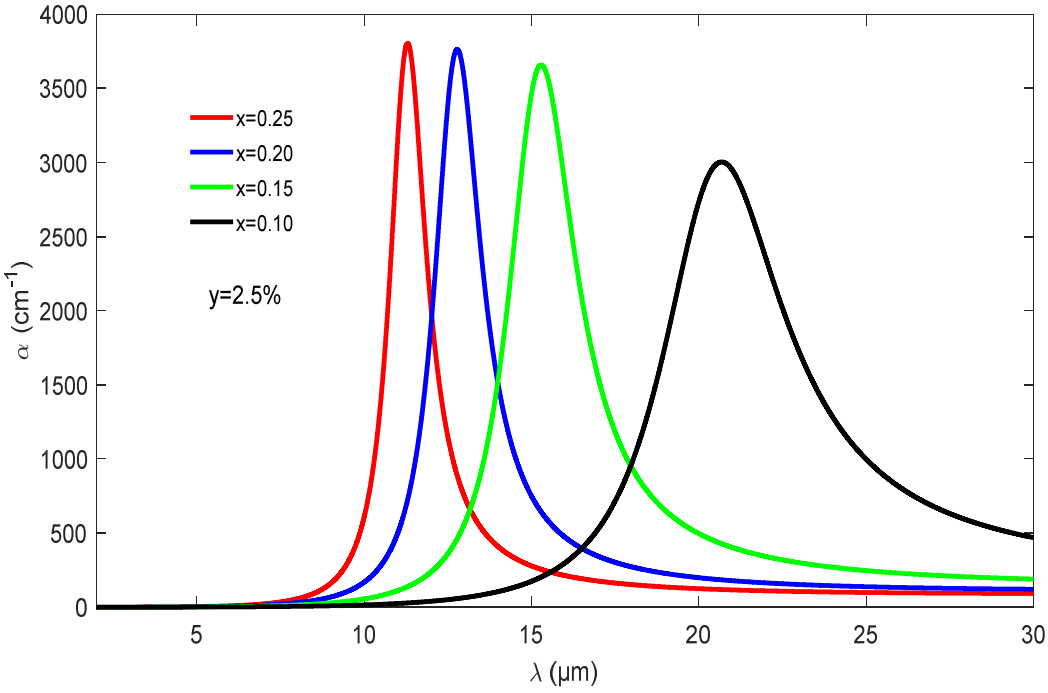


Figure 8

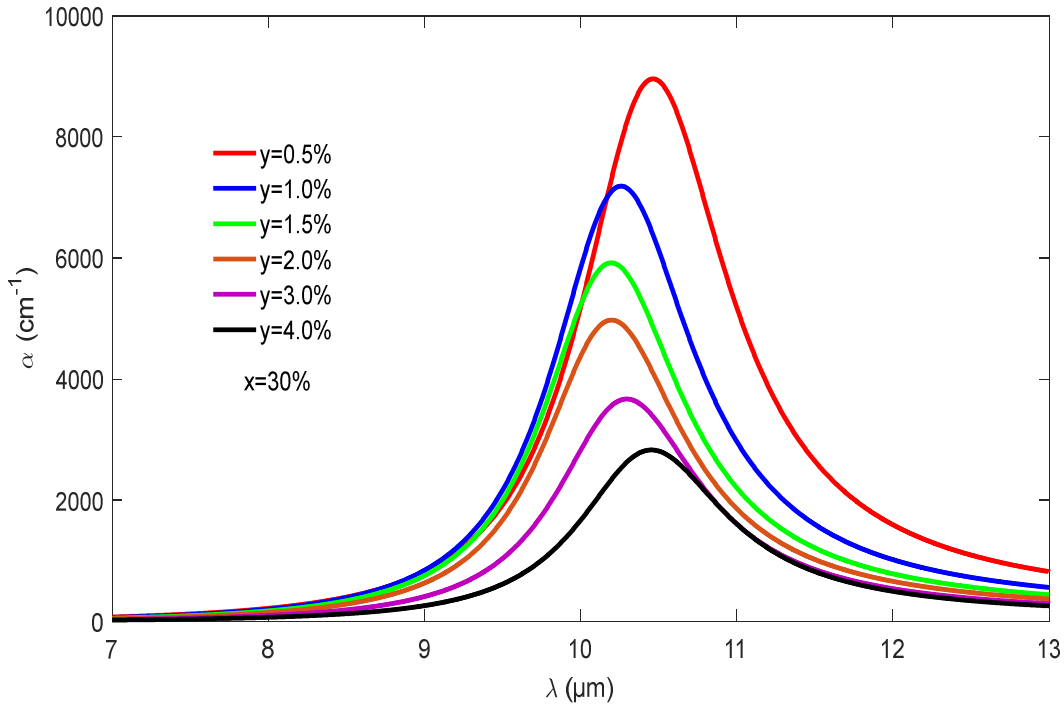


Figure 9

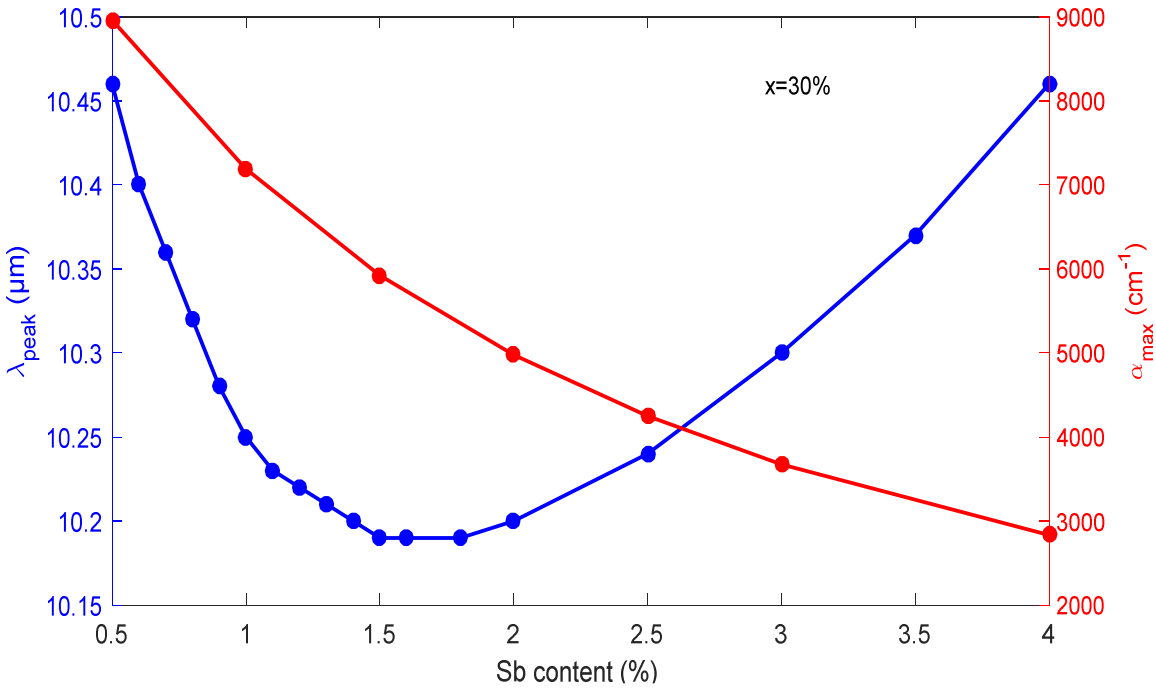


Figure 10

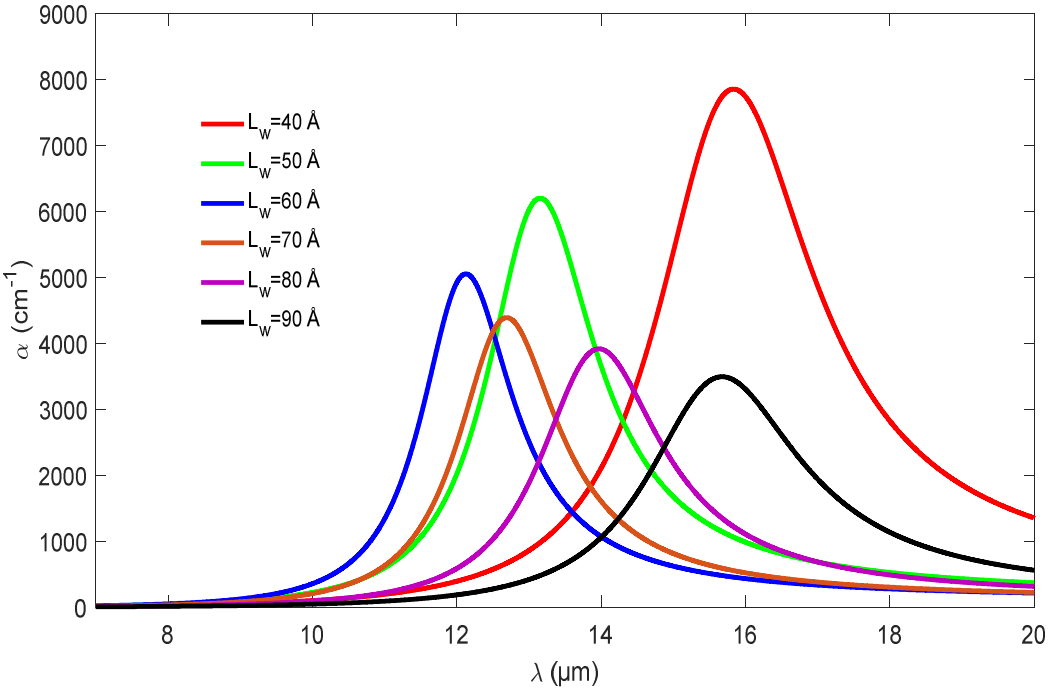


Figure 11

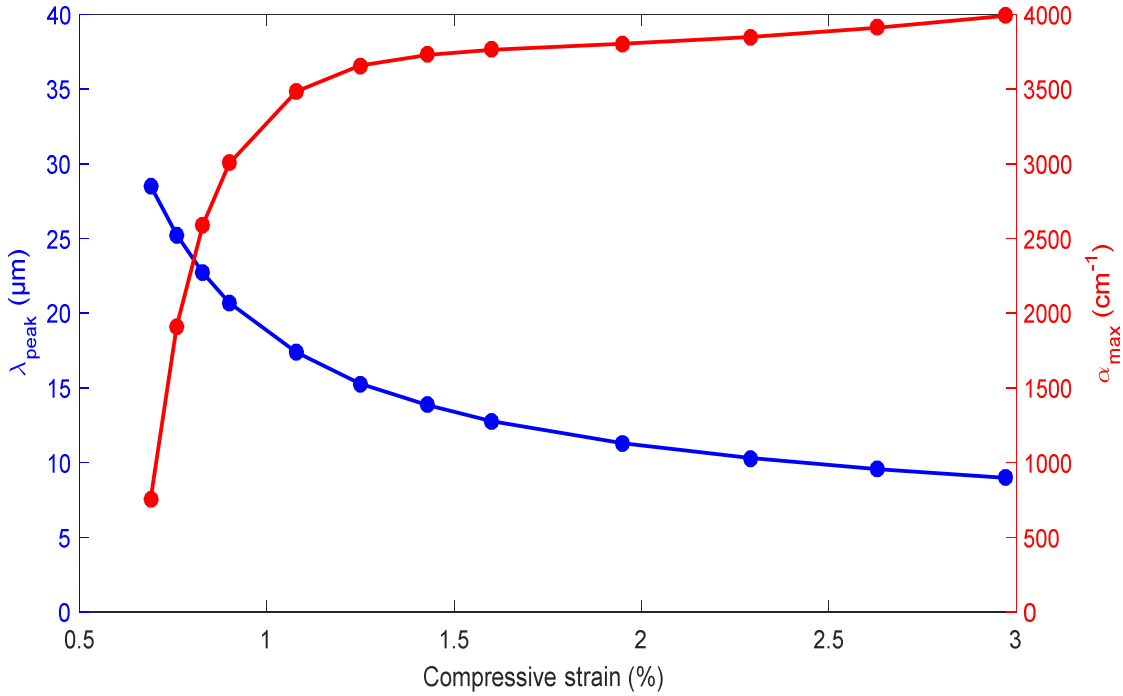


Figure12